Proceedings of the 7th World Congress on Civil, Structural, and Environmental Engineering (CSEE'22)
~~Lisbon, Portugal~~ Virtual Conference – April 10 – 12, 2022
Paper No. ICGRE 140
DOI: 10.11159/icgre22.140

Numerical Study of A Deep Cut Slope Stabilization in Residual Soil

X.C Lin[1]
[1]Virtuosity, Bentley System(s)
Singapore city, Singapore
xc.lin@bentley.com

***Abstract* -** This paper presents the numerical analysis of soil-nail reinforced deep slope cut, for the construction of student hostels at National University of Singapore. The reinforcement system of soil nails was represented by 2D/ 3D Embedded Beam (Row) model in PLAXIS, the performance of which was investigated by drawing comparison against available field data over various geotechnical aspects, e.g. slope deformation, pull-out resistance, and axial response of soil nails, followed by a discussion on the factor of safety obtained in Finite Element Method (FEM) and Limit Equilibrium Method (LEM), that further validated the model and its applicability, as well as how the use of FEM could complement conventional design methods in achieving economical yet reliable design. It has further affirmed that, in the absence of a 3D program, 2D program can effectively handle groups of soil nails in the plane strain condition and produce both quantitative and qualitative predictions of deformation and structural response that concerns practitioners.

***Keywords*:** Soil Nail, Pull-out Test, Slope, FEM, LEM, Safety, Embedded Beam, PLAXIS

1. Introduction

The proposed student hostels were constructed in a shallow valley, along Prince George's Park (PGP) Road in National University of Singapore. According to the existing ground profile, only two sides of the excavation needed to be stabilized, being the one along PGP Road and the other on the north-eastern side. The study focused on the stabilization works for the cut slope along PGP Road, as it was more critical based on the length and height.

The proposed but slope along PGP Road was 240 m long and 10.7 m to 13.6 m high. As shown in Fig.1, it was divided into 11 zones according to the propose building layout, whereby slopes in zone 2, 4, 6 and 8 were the steeper, with inclination of 74^0 to 77^0, as compared to slopes in zone 1, 3, 5 and 7, with inclination of 36^0 to 55^0.

2. Ground Conditions

The site was located in the south-western part of Singapore. The geological formation is Jurong Formation, where the subsoil is predominantly residual soil of sedimentary origin. (3) boreholes, BH2A, 3A and 5, as shown in Fig.2, had been sunk along the PGP Road before excavation, to explore the subsurface soil conditions. The focus of this study was Section 1-1 in Zone-2, where BH3A was deemed to provide the most relevant subsoil information. It suggested a 4-layer profile consisting of medium stiff clayed silt, overlying medium to dense sand and weathered sandstone.

The pore water pressure was monitored along the slope, by (7) pneumatic piezometers installed along the PGP Road. The phreatic surface was found to vary with weather and excavation levels, with the highest water table found at the north-western corner, where run-off water from the western hill maintained the water table at about 4.5 m below ground surface, and the general trend of the phreatic surface followed the ground surface profile, sloping down towards the south.

3. FEM Modelling

3.1. Geometry

Both the 2D and 3D models are shown in Fig.3, whereby in 3D model we consider a slice equal to the soil-nail spacing.

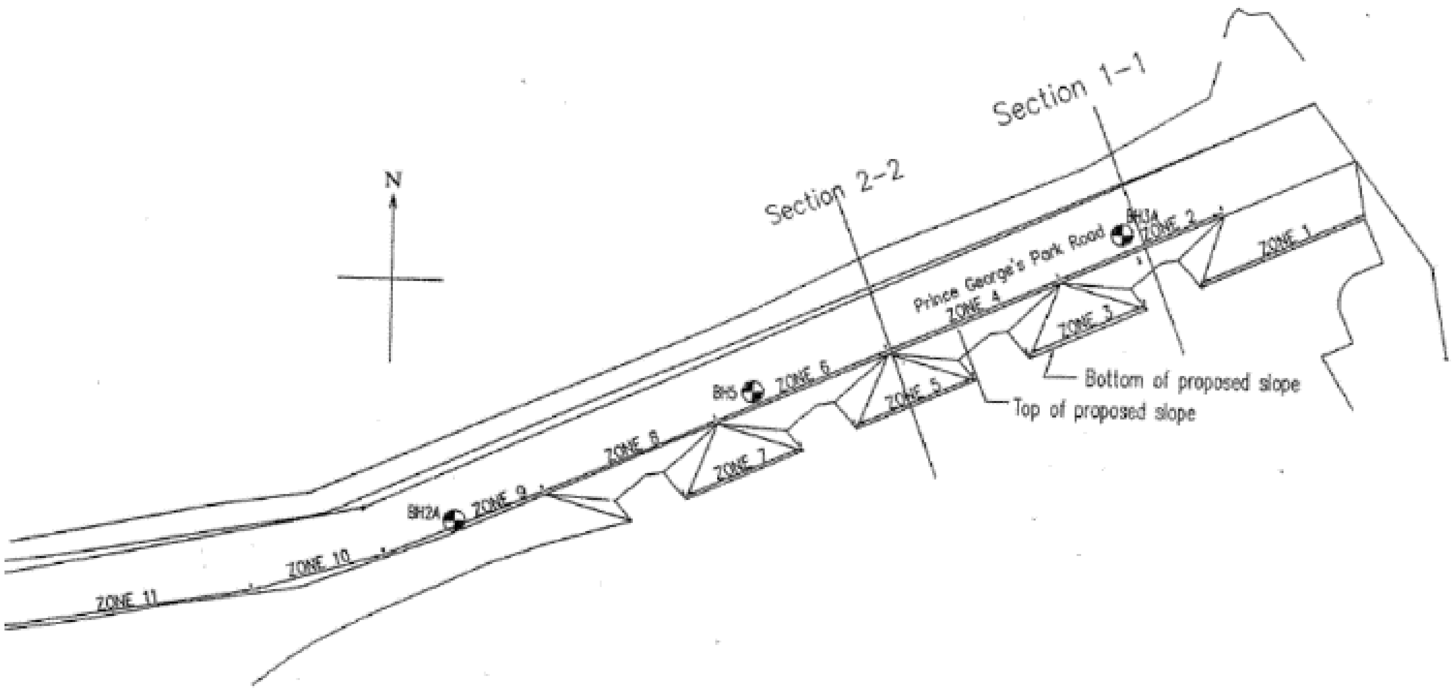

Fig. 1: Site layout and borehole locations

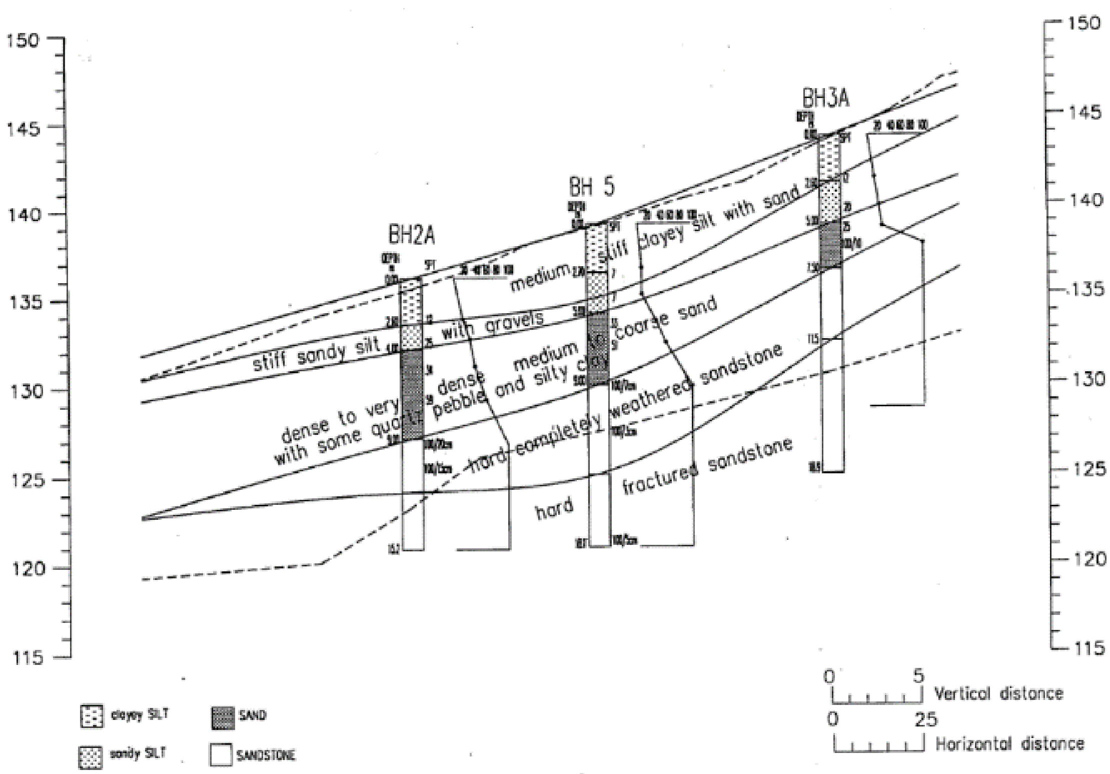

Fig. 2: Soil profile

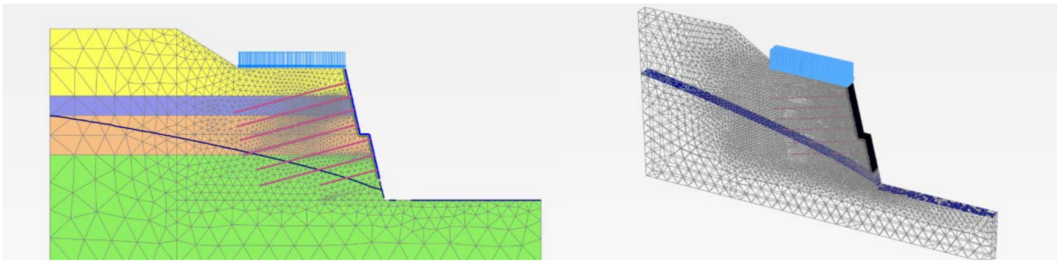

Fig. 3: 2D and 3D models

3.2. Soil Parameters

The subsoil was divided into (4) layers based on the soil investigation. The first layer of soil, from ground surface to a depth of 2.6 m on average, was medium stiff clayey silt; the Standard Penetration Test (SPT) blow counts varied from 7 to 12, giving an average value of 10. The second layer consisted of medium dense to very dense sand, with trace of quartz pebble, in the depth of 2.6 m to 9 m where SPT increases from 12 to 59 with an average value of 41. These two layers of soils were residual soils formed by weathering of the underlying bedrocks. The third layer, below 9 m, was completely weathered sandstone, with SPT blow counts at 100 or over.

In this study, advanced soil model, e.g. Hardening Soil with Small Strain Stiffness (HSsmall) model was used. HSsmall model is an extension of Hardening Soil model, with an elastic overlay model to account for the high stiffness at small strain levels. The model requires the input of (3) stiffness parameters, of E_{50}^{ref}, E_{oed}^{ref} and E_{ur}^{ref}, that controls the deformation behavior of the soil under deviatoric loading, volumetric loading and unloading, respectively. Experience suggested that the correlation of $E = N$, e.g. with N being the SPT blow counts, would produce good resolution of the soil deformation behavior as observed in the field, for the geological formation. The $E_{ur}^{ref}/\ E_{oed}^{ref}$ ratio usually falls in the range of 3 to 5 for the material, here a lower bound of 3 was considered, which was in line with Brinkgreve [1]. In addition, it requires (2) additional parameters of G_0 and $\gamma_{0.7}$, to describe the small strain behavior. The $G_0/\ G_{ur}$ ratio for different types of geomaterial falls in the range of 2.5 to 10, according to Brinkgreve [2]. The $\gamma_{0.7}$ can be deduced based on the Brinkgreve [3] correlation as follows,

$$\gamma_{0.7} \approx \frac{1}{9G_0}\left[2c'(1+\cos 2\varphi') + \sigma'_1(1+k_0)\sin 2\varphi'\right] \tag{1}$$

The input soil parameters are summarized in Table.1.

Table 1: Input soil parameters

Descriptions.	E_{50}^{ref}, kPa	E_{oed}^{ref}, kPa	E_{ur}^{ref}, kPa	*m* -	*c*, kPa	*φ'* °	*ψ* °	G_0, kPa	$\gamma_{0.7}$ -
Med. Stiff Clayed Silt	7,000	7,000	21,000	0.5	7	28	0	84,000	1.97E-4*/ 2E-4
Med. Dense Sand	10,000	10,000	30,000	0.5	3	30	0	85,000	1.82E-4*/ 2E-4
Dense Sand	20,000	20,000	60,000	0.6	3	40	10	93,000	1.67E-4*/ 2E-4
Sandstone II	100,000	100,000	300,000	0.6	7	40	10	300,000	5.53E-5*/ 2E-4

* - *Brinkgreve [3]*

3.3. Soil-nail Parameters

(6) numbers of soil nails were installed for the pull-out test; of which (5) were installed in Zone-1 where slope was highest and steepest, and (1) in Zone-6, in the middle of the 240 m long slope. The structural response, in particular the mobilization of skin friction, is dependent on the complex soil-structure interaction, which is a result of the constitutive response of the chosen soil model to equilibrium. The key to a realistic numerical structure response, greatly depends accurate input skin resistance profile, besides the appropriate parameters used in the constitutive soil model. Pull-out tests were simulated in PLAXIS 2D and 3D, as shown in Fig.3, at the same stress level, to understand the numerical capacity of the soil-nail modelled. It turned out the numerical response was well below the field results. A corrected skin friction of 148 kPa was therefore adopted for input. Field and numerical pull-out test curves are shown in Fig.4.

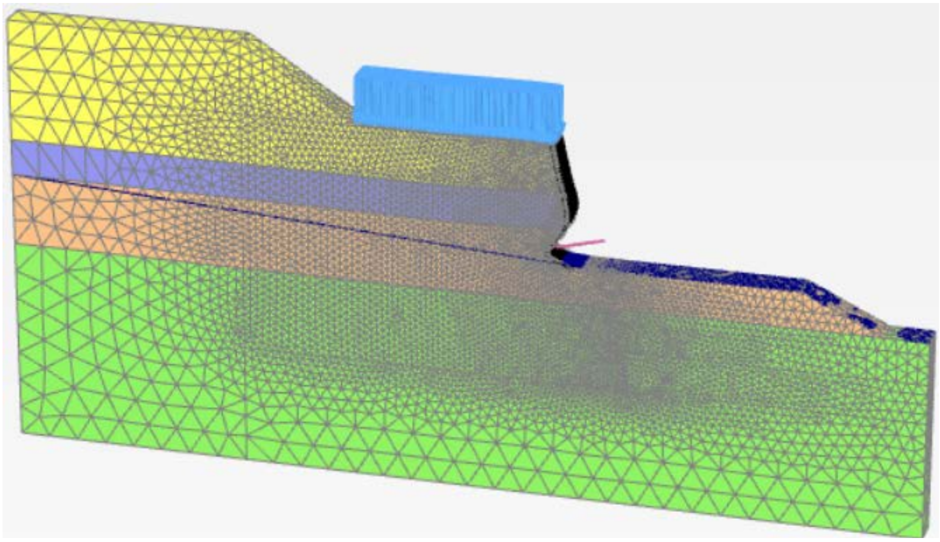

Fig. 3: Numerical pull-out test

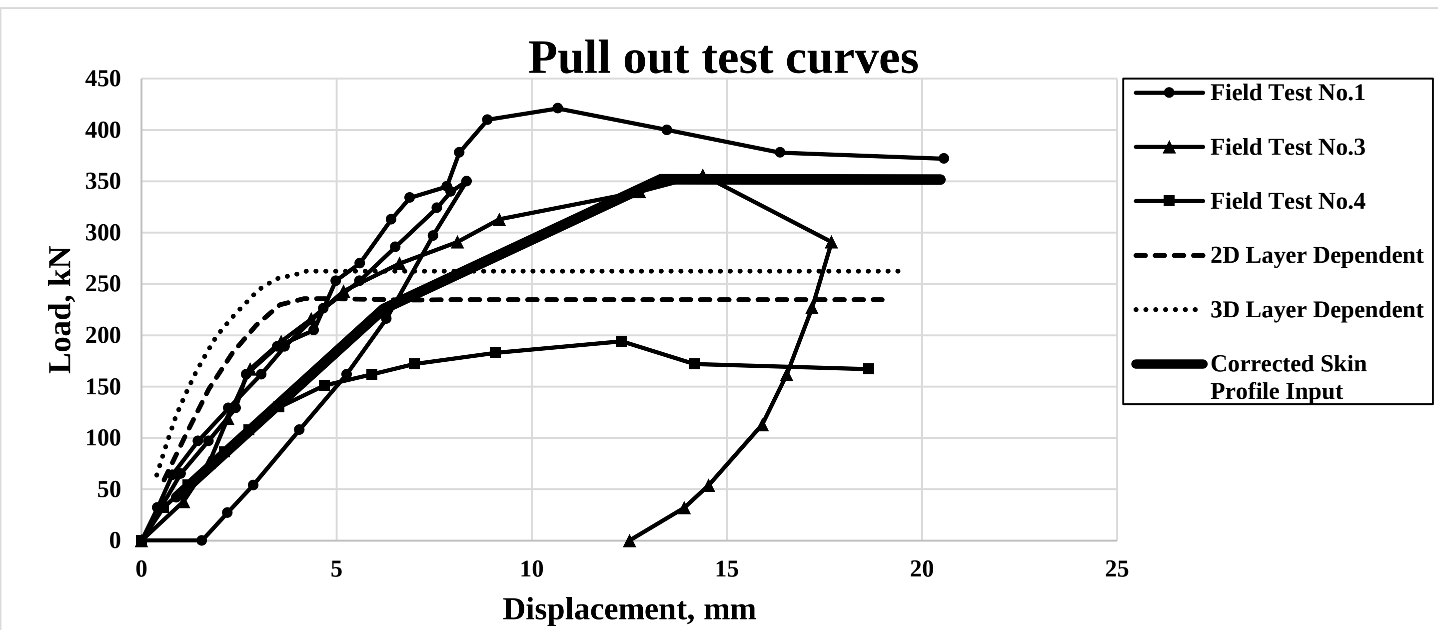

Fig. 4: Field and numerical pull-out test curves

Table 2: Input properties for soil nails

Description.	*E*, kPa	*γ*, kN/m³	*d*, mm	$L_{spacing}$, m	*Skin Resistance*	T_{max}, kN/m
Soil Nail	30E6	3	140	1.60	Linear	65

3.4. Parameters for Shotcrete Facing

The designed guniting facing thickness was in the range of 80 to 100 mm and the steel meshes were one layer of steel mesh D8, two layers of D6 (σ_y = 460 N/mm^2) or their combination, depending on the location. The shotcrete facing was modelled using *plate* element in PLAXIS, with the input properties summarized in Table.3.

Table 3: Input properties for shotcrete facing

Description.	*EA*, kN/m	*EI*, kNm²/m	*w*, kN/m/m	*d*, mm	*ν* -
Facing	3E6	2500	0.4	100	0.2

3.5. Staged Constructions

The construction works involved (6) steps in following sequence: excavation, fixing steel meshes, guniting, drilling of boreholes, installation of nails, grouting and casting soil nail heads.

Excavation was carried out in stages, and the excavation depth at each stage was determined by the vertical spacing between the levels of the current and next layer of soil nails. The construction progress is summarized in Table.4.

Table 4: Excavation schedule

Date	22/6	6/7	5/8	11/8	19/8	26/8
Excavation depth (m)	2.5	4.8	6.8	8.9	11.2	13.6

4. FEM Results

4.1. Horizontal Movements at Facing

The lateral displacements were monitored by the (7) inclinometers, at different excavation stages. The horizontal deflection profiles by PLAXIS 2D, 3D and field measurement for each excavation stage, so was the envelope profile with movement maxima and minima throughout all excavation stages, were charted in Fig.5.

During the open cut of the first 2.5 m, 3D predicted excessive movement as compared to 2D and field response. This was due to some convergence issues in the 3D analysis in that stage, where the program resorted to more displacement for equilibrium. Similar issues were observed for the subsequent stages, that potentially gave rise to the discrepancies between 2D and 3D prediction. It’s worth to note that FEM results are mesh-dependent, and during the setup of 3D model, additional mesh refinement was applied, to compensate the shortfall in accuracy, between 3D tetrahedral element (2nd order), and the 15 noded 2D element (4th order). In general, a denser mesh discretization gives better resolution in results, yet in the meantime, convergence issues might arise from the localized failure mechanisms developed, and sometimes such mechanisms are geotechnically irrelevant. The match between 2D and 3D could be improved through further optimization in the 3D mesh. In this case, 2D prediction gave better match with field data, due to less impact from the aforementioned issue, as compared to 3D prediction.

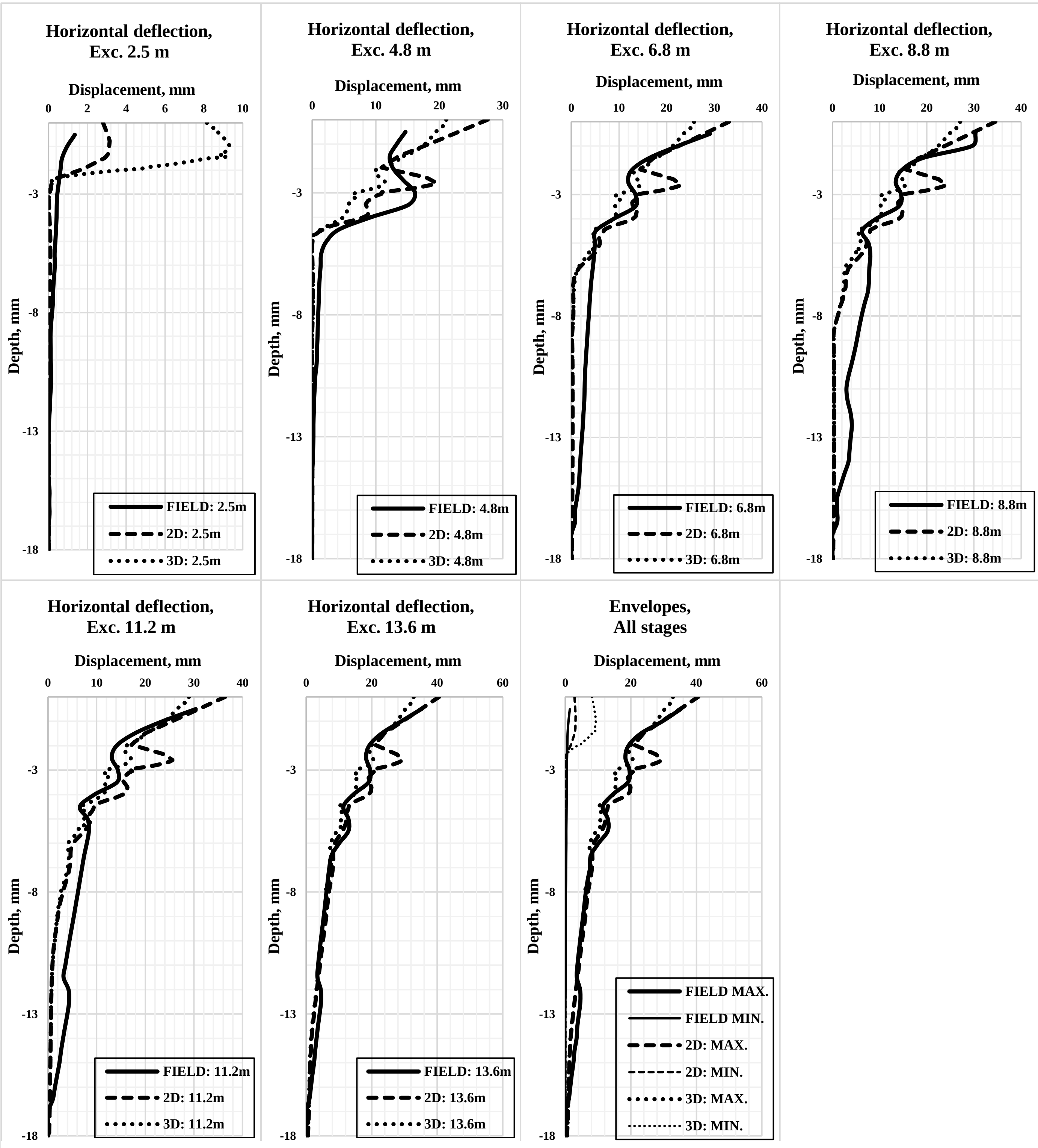

Fig. 5: Horizontal deflection profile and envelopes at all excavation stages

4.2. Axial Forces of Soil Nails

Strain gauges were installed for Nail 1, 4 and 7, at a spacing varying from 1.5 m to 2 m. Complete filed measurement was only available for Nail-1, as shown in Fig.6. It turned out that, numerical analysis underpredicted the axial force in the active zone, e.g. close to the facing, while better match was found towards the passive zone. A plausible explanation is that the facing was more rigid than what was modelled, e.g. the interaction of the soil nail bar and the bearing plate at the fixed joint, cannot be fully captured with the simple structural elements used in the analysis.

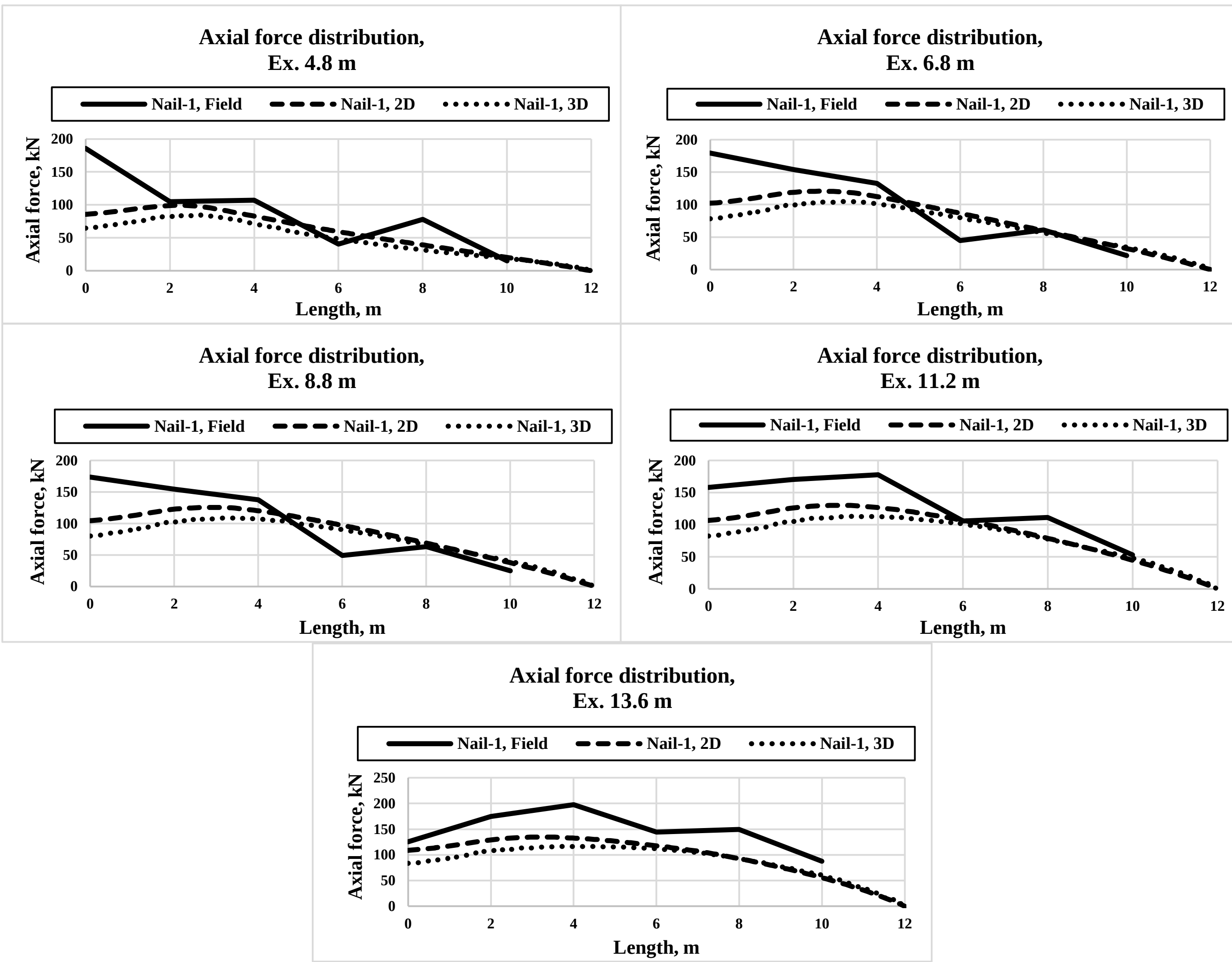

Fig. 6: Axial force distribution of Nail-1 throughout the stages

5. Factor of Safety

The original design of the reinforcement for stabilization of the cut slopes, was based on limit equilibrium concept. It considered the strength limit state by ensuring that the combined strength of the nails and the soil, exceeded the applied load, with a factor of safety appropriate to the level of uncertainty associated with the loads due to the excavation. Gässler [4] stated that for less steep slope, < 80°, the critical mechanism might be a circular slip surface. The design of the optimum soil nail arrangement was obtained by adjusting soil nail spacing, until the factor of safety met the required minimum of 1.5.

Global factor of safety (LEM) was checked according to the forces on soil nail related to a circular potential failure surface, according to Luo [5].

In PLAXIS, the factor of safety is evaluated through an artificial process, that progressively reduces the strength of the soil, to trigger the failure. In this case, PLAXIS 2D and 3D predicted the safety factor of 1.498 and 1.497, respectively, as shown in Fig.7, that were sufficiently close to 1.5, which the design was originally based off.

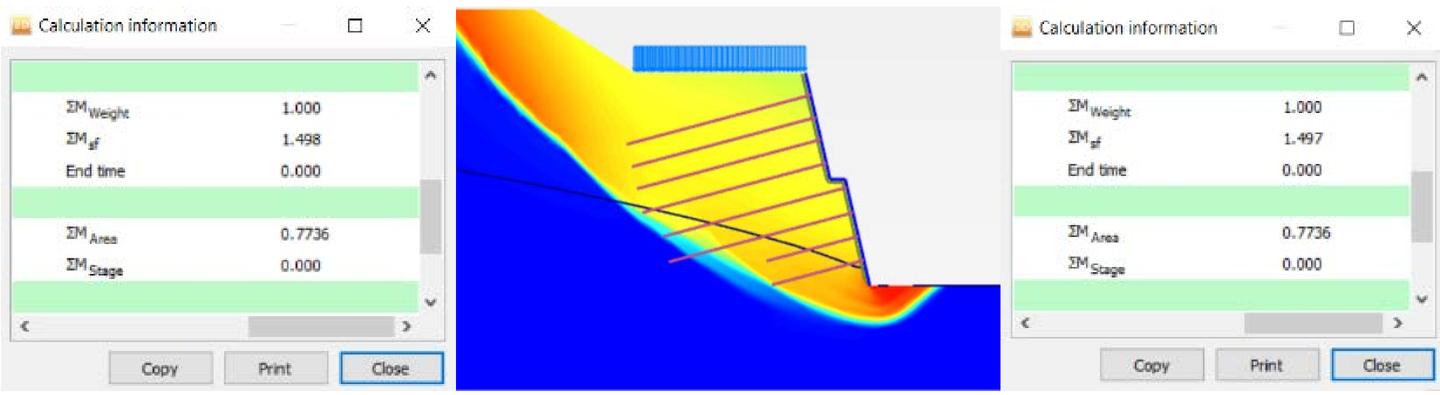

Fig. 7: Safety factor and failure mechanism by PLAXIS

6. Conclusions

Geotechnical designs are driven by both serviceability and stability concerns; and quite often, designs are governed by the serviceability criterion. Traditional designs based on LEM is adequate, but the efficiency is questionable due to the lack of knowledge in soil-structure interaction, e.g. a factor of safety is not going to help us in understanding the response of the geo-structure, at least under the service or working condition. This study demonstrated how the use of FEM could complement conventional methods, in achieving economical and reliable designs. Although the structural element like *embedded beam (row)* in the PLAXIS code comes in handy, in representing the soil-nail group behaviours, care should be taken to validate the numerical response against available field data, the idea is to ensure that we do not overpredict the pull-out resistance in the analysis. Numerical results, on the other hand are mesh-dependent, it is worth to invest some effort in optimizing the mesh discretization and finetuning local behaviours, through an iterative process.

References

[1] R. B. J. Brinkgreve and E. Engin and H. K. Engin, “Validation of empirical formulas to derive model parameters for sands,” in *Proceedings of the 7th European Conference on Numerical Methods in Geotechnical Engineering, NUMGE*, Trondheim, Norway, 2010, vol. 1, pp. 137-142.

[2] R. B. J. Brinkgreve and M. H. Kappert and P. G. Bonnier, “Hysteretic damping in a small-strain stiffness model,” in *Numerical Models in Geomechanics*, Pande & Pietruszczak, Ed. London: Taylor & Francis Group, 2007.

[3] R. B. J. Brinkgreve and S. Kumarswamy and W. M. Swolfs and F. Foria, “The hardening soil model with small-strain stiffness (HSsmall),” in *PLAXIS 2D Material Models Manual*, Netherlands: Plaxis bv, 2018, pp. 92.

[4] G. Gässler, “Soil nailing theoretical bars and practical design,” in *Proceedings of the International Geotechnical Symposium on Theory and Practice of Earth Reinforcement*, Fukuoka, Japan, 1988, vol. 1, pp. 283-288.

[5] S. Q. Luo, “Soil nail behaviors,” Ph.D. dissertation, Dept. Civil. Eng., National University of Singapore.